Mach-Zehnder modulator based octupling optical MM-wave 4PSK signal generation for RoF links

XIAOGANG CHEN[a,b,*], ZHENGOU HUANG[b]
[a]*School of Electrical and Photoelectronic Engineering, Changzhou Institute of Technology, Changzhou, Jiangsu, 213032, China*
[b]*Nanfang Communications Technology Corporation Limited, Changzhou, Jiangsu, China*

Two novel approaches without optical filtering are proposed for octupling optical millimeter-wave (MM-wave) 4PSK vector signal generation, one is based on dual-parallel Mach-Zehnder modulator (DPMZM) and the other is based on integrated MZM. Theoretical analysis and simulation experiments are demonstrated for the two octupling schemes. In DPMZM based scheme, only the +4th-order sideband is modulated by data signal and the -4th-order sideband is un-modulated. While in integrated MZM based approach, only the +3rd-order sideband is modulated by data signal and the -5th-order sideband is un-modulated. RoF Links based on the two proposed schemes are established and 2.5 Gbit/s data transmission performances are evaluated. Both schemes can transmit the generated optical MM-wave 4PSK signal up to 30 Km at BER = 10^{-9}, and the receiver sensitivity of DPMZM based approach is superior to that of integrated MZM based approach.

(Received February 27, 2020; accepted June 16, 2020)

Keywords: Microwave Photonics, Radio over Fiber (RoF), Frequency octupling, Mach-Zehnder modulator (MZM)

1. Introduction

With the increasing development of broadband wireless access (BWA) services, millimeter-wave (MM-wave) communication becomes a powerful technology with its high speed and bandwidth. However, the transmission loss of high frequency MM-wave in free space is quite large and its coverage is very limited. Due to the large bandwidth and low transmission loss of optical fiber, Radio over fiber (RoF) technology combines the advantages of optical fiber and wireless communication, providing a promising path for future BWA networks [1,2].

For RoF system that service BWA networks, the effective generation of high frequency optical MM-wave is a crucial factor [3,4]. Nevertheless, owing to the limited frequency responses of optical and electrical elements, it is difficult to directly generate optical MM-wave of 60 GHz or above. Therefore, it is of important implication to explore frequency multiplication technique to generate high frequency optical MM-wave. Some frequency multiplication based optical MM-wave generating mechanisms have been outlined [5-8], among them, the approach based on Mach-Zehnder modulator (MZM) including dual-parallel MZM [9,10] has attracted a lot of attention. However, due to the nonlinear transformation from frequency multiplication, the above schemes are not appropriate for generating vector modulation formats including multiple phase shift keying (MPSK) and orthogonal amplitude modulation (QAM), which are critical to wireless communication. Such methods for generating optical MM-wave vector signals are raised [11,12]. However, using wavelength selection switches (WSS) [8] or optical filter [11] to eliminate the unwanted optical sidebands will enhance system complexity and block the realization of WDM-RoF systems.

In the paper, without optical filtering, octupling optical MM-wave 4PSK signal generation scheme base on dual-parallel MZM (DPMZM) and integrated MZM is presented, respectively. Base on the above two approaches, the transmission performances for 2.5 Gbit/s RoF links at 80 GHz band are assessed, 4PSK optical MM-wave signal could be distributed 30 Km at BER = 10^{-9}.

2. Principle

The block diagram of RoF link based on DPMZM and integrated MZM is plotted in Fig. 1(a) and Fig. 1(b), respectively. The lightwave from laser diode (LD) is expressed as $E_0 e^{j\omega_0 t}$, E_0 and ω_0 are amplitude and angular frequency of the optical carrier, respectively. The local radio frequency (RF) signal is modulated by the binary data signal $d(t)=\sum_n I_n g(t-nT)$ via an electrical phase modulator (PM). Here, I_n is the binary digital signal of the 0-1 sequence, T is the symbol period, and g(t) is the symbol form function. Both the DPMZM and integrated MZM are driven by the phase modulated signal and the electrical gained signal of d(t). A $\pi/2$ phase shift is applied between two arm driving RF signals of DPMZM and integrated MZM, and a π phase difference is introduced between upper and lower arm of each sub-MZM.

2.1. DPMZM based RoF link

The DPMZM is made of two parallel sub-MZMs (MZM1 and MZM2), and both of two sub-MZMs are

biased at the full point. The input RF signal of MZM1 and MZM2 can be indicated as $V_1(t) = V_m \sin[\omega_m t + \pi/16 d(t)] + 1/4 V_\pi d(t)$ and $V_2(t) = V_m \sin[\omega_m t + \pi/16 d(t) + \pi/2] + 1/4 V_\pi d(t)$, respectively. Where V_m and ω_m are amplitude and angular frequency of local RF signal, respectively. V_π is the half-wave voltage of sub-MZM. Therefore, the optical MM-wave at the output of MZM1 can be represented as

$$E_1(t) = \frac{E_0}{4} e^{j\omega_c t}[e^{j\frac{\pi\{[V_m \sin[\omega_m t+\frac{\pi}{16}d(t)]+\frac{1}{4}V_\pi d(t)\}}{V_\pi}} + e^{j\frac{\pi\{V_m \sin[\omega_m t+\frac{\pi}{16}d(t)+\pi]+\frac{1}{4}V_\pi d(t)\}}{V_\pi}}]$$
$$= \frac{E_0}{4} e^{j\omega_c t} \sum_{n=-\infty}^{\infty} J_n(m) e^{jn[\omega_m t+\frac{\pi}{16}d(t)]}(1+e^{jn\pi}) e^{j\frac{\pi}{4}d(t)} \quad (1)$$

where $m = \pi V_m / V_\pi$ is modulation index (MI) of each sub-MZM, and $J_n(x)$ is the n order Bessel function of the first kind.

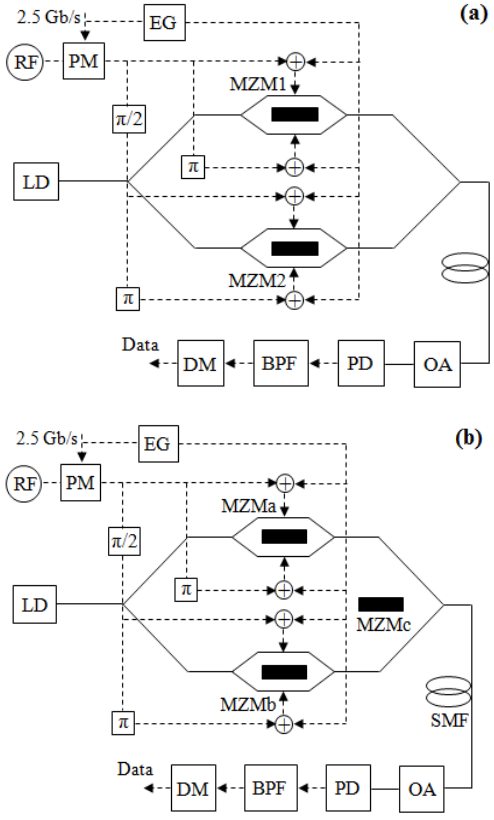

Fig. 1. Block diagrams of two RoF links. (a) DPMZM based, (b) Integrated MZM based. LD: laser diode; RF: radio frequency; PM: electrical phase modulator; EG: electrical gain; MZM: Mach-Zehnder Modulator; SMF: single mode fiber; OA: optical amplifier; PD: photo diode; BPF: bandpass filter; DM: electrical phase Demodulator

Similarly, the output optical MM-wave from MZM2 is

$$E_2(t) = \frac{E_0}{4} e^{j\omega_c t}[e^{j\frac{\pi\{[V_m \sin[\omega_m t+\frac{\pi}{16}d(t)+\frac{\pi}{2}]+\frac{1}{4}V_\pi d(t)\}}{V_\pi}} + e^{j\frac{\pi\{V_m \sin[\omega_m t+\frac{\pi}{16}d(t)+\frac{3\pi}{2}]+\frac{1}{4}V_\pi d(t)\}}{V_\pi}}]$$
$$= \frac{E_0}{4} e^{j\omega_c t} \sum_{n=-\infty}^{\infty} J_n(m) e^{jn[\omega_m t+\frac{\pi}{16}d(t)]}(1+e^{jn\pi}) e^{jn\frac{\pi}{2}} e^{j\frac{\pi}{4}d(t)} \quad (2)$$

As a consequence, the optical MM-wave generated by DPMZM can be written as

$$E_D(t) = E_1(t) + E_2(t)$$
$$= \frac{E_0}{4} e^{j\omega_c t} \sum_{n=-\infty}^{\infty} J_n(m) e^{jn[\omega_m t+\frac{\pi}{16}d(t)]}[1+(-1)^n](1+e^{jn\frac{\pi}{2}}) e^{j\frac{\pi}{4}d(t)}$$
$$= \frac{E_0}{2} e^{j\omega_c t} \sum_{n=-\infty}^{\infty} J_n(m) e^{j4k[\omega_m t+\frac{\pi}{16}d(t)]}(1+e^{j4k\frac{\pi}{2}}) e^{j\frac{\pi}{4}d(t)} \quad (3)$$

According to formula (3), 4k[th] -order harmonics are produced by the DPMZM. As bessel function $J_n(m)$ decrease with the increasing of order n, so it is logical to neglect optical sidebands of order 8[th] and above in the analysis. In order to suppress optical carrier, MI could be set to 2.4048 (m = 2.4048), and the optical MM-wave from DPMZM could be reduced to

$$E_D(t) = E_0 J_4(m) e^{j\omega_c t}\{e^{-j[4\omega_m t+\frac{\pi}{4}d(t)]} + e^{j[4\omega_m t+\frac{\pi}{4}d(t)]}\} e^{j\frac{\pi}{4}d(t)}$$
$$= E_0 J_4(m) e^{j\omega_c t}\{e^{-j4\omega_m t} + e^{j[4\omega_m t+\frac{\pi}{2}d(t)]}\} \quad (4)$$

The optical MM-wave produced by DPMZM mainly includes +4[th] and -4[th]-order optical sidebands, in which only +4[th]-order sideband is modulated by data while -4[th]-order sideband is un-modulated. When d(t) is 0 or 1, the phase of +4[th]-order carrying data sideband is 0 or π/2 respectively, so 4PSK vector signal is produced. Since photo diode (PD) probes the received signal by square law detection, the beating between +4[th] and -4[th]-order harmonics produces an 8-fold MM-wave signal.

2.2. Integrated MZM based RoF link

The integrated MZM consists of three sub-MZMs (MZMa, MZMb and MZMc). Both MZMa and MZMb are biased at the null point, MZMc is biased at quadrature point to introduce π/2 phase difference between outputs from MZMa and MZMb. The input signal of MZMa and MZMb can be indicated as $V_a(t) = V_m \sin[\omega_m t + \pi/16 d(t)] + 5/16 V_\pi d(t)$ and

$V_b(t) = V_m \sin[\omega_m t + \pi/16 d(t) + \pi/2] + 5/16 V_\pi d(t)$, respectively. Therefore, the optical MM-wave at the output of MZMa can be represented as

$$E_a(t) = \frac{E_0}{4} e^{j\omega_c t}[e^{j\frac{\pi\{[V_m \sin[\omega_m t+\frac{\pi}{16}d(t)]+\frac{5}{16}V_\pi d(t)+V_\pi\}}{V_\pi}} + e^{j\frac{\pi\{V_m \sin[\omega_m t+\frac{\pi}{16}d(t)+\pi]+\frac{5}{16}V_\pi d(t)\}}{V_\pi}}]$$

$$= \frac{E_0}{4} e^{j\omega_c t} \sum_{n=-\infty}^{\infty} J_n(m) e^{jn[\omega_m t+\frac{\pi}{16}d(t)]} (e^{jn\pi} - 1) e^{j\frac{5\pi}{16}d(t)} \quad (5)$$

Similarly, the output optical MM-wave from MZMb is

$$E_b(t) = \frac{E_0}{4} e^{j\omega_c t}[e^{j\frac{\pi\{[V_m \sin[\omega_m t+\frac{\pi}{16}d(t)+\frac{\pi}{2}]+\frac{5}{16}V_\pi d(t)+V_\pi\}}{V_\pi}} + e^{j\frac{\pi\{V_m \sin[\omega_m t+\frac{\pi}{16}d(t)+\frac{3\pi}{2}]+\frac{5}{16}V_\pi d(t)\}}{V_\pi}}]$$

$$= \frac{E_0}{4} e^{j\omega_c t} \sum_{n=-\infty}^{\infty} J_n(m) e^{jn[\omega_m t+\frac{\pi}{16}d(t)]} (e^{jn\pi} - 1) e^{j\frac{\pi}{2}} e^{j\frac{5\pi}{16}d(t)} \quad (6)$$

As a consequence, the optical MM-wave generated by integrated MZM can be written as

$$E_I(t) = E_a(t) + E_b(t) e^{jn\pi/2}$$

$$= \frac{E_0}{4} e^{j\omega_c t} \sum_{n=-\infty}^{\infty} J_n(m) e^{jn[\omega_m t+\frac{\pi}{16}d(t)]} [(-1)^n - 1](1 + e^{j(n+1)\frac{\pi}{2}}) e^{j\frac{5\pi}{16}d(t)}$$

$$= \frac{E_0}{2} e^{j\omega_c t} \sum_{n=-\infty}^{\infty} J_n(m) e^{j(4k+3)[\omega_m t+\frac{\pi}{16}d(t)]} [1 + e^{j(4k+4)\frac{\pi}{2}}] e^{j\frac{5\pi}{16}d(t)} \quad (7)$$

According to formula (7), 4k+3[th] -order harmonics are produced by the DPMZM. It is logical to neglect optical sidebands of order 7[th] and above in the analysis. In order to suppress -1[st] -order harmonic, MI could be set to 3.8317 (m = 3.8317), and the optical MM-wave from integrated MZM could be reduced to

$$E_I(t) = E_0 e^{j\omega_c t}\{J_3(m) e^{j[3\omega_m t+\frac{3\pi}{16}d(t)]} - J_5(m) e^{-j[5\omega_m t+\frac{5\pi}{16}d(t)]} - \} e^{j\frac{5\pi}{16}d(t)}$$

$$= E_0 e^{j\omega_c t}\{J_3(m) e^{j[3\omega_m t+\frac{\pi}{2}d(t)]} - J_5(m) e^{-j5\omega_m t}\} \quad (8)$$

The optical MM-wave produced by integrated MZM mainly includes +3[rd] and -5[th]-order optical sidebands, in which only +3[rd] -order sideband is modulated by data while -5[th]-order sideband is un-modulated. When d(t) is 0 or 1, the phase of +3[rd]-order carrying data sideband is 0 or π/2 respectively, so 4PSK vector signal is produced. Similarly, the beating between +3[rd] and -5[th]-order harmonics produces an 8-fold MM-wave signal.

3. Results and discussion

To assess the feasibility of the two devised octupling optical MM-wave 4PSK signal generation schemes as shown in Fig. 1, simulation experiment was executed based on OptiSystem software and the corresponding parameters were consistent with the theoretical values. The frequency of driving RF signal is 10 GHz and the lightwave frequency at the our of LD is 193.1 THz. The insert loss and half-wave voltage of each sub-MZM is 5 dB and 4 V, respectively. 2.5 Gbit/s data carried by the generated 4PSK optical MM -wave are transmitted over single mode fiber (SMF), whose dispersion and attenuation coefficient is 16.75 ps/nm/km and 0.2 dB/ km, respectively. The received optical power of RoF link is sustained by an optical amplifier (OA), whose gain and noise figure is 20 dB and 4 dB, respectively. With square law detection, a PD of 0.8 A/ W responsivity, 10 nA dark current and 1e-22 W/Hz thermal power density is used to examine the received signal. The target data spectrum is selected from the detected signal by an electrical band pass filter (BPF), whose bandwidth is 1.5 times the data rate. Then an electrical phase demodulator (DM) is adopted to demodulate the filtered signal. Finally, system performance of the RoF link is tested by a bit-error-rate (BER) analyzer.

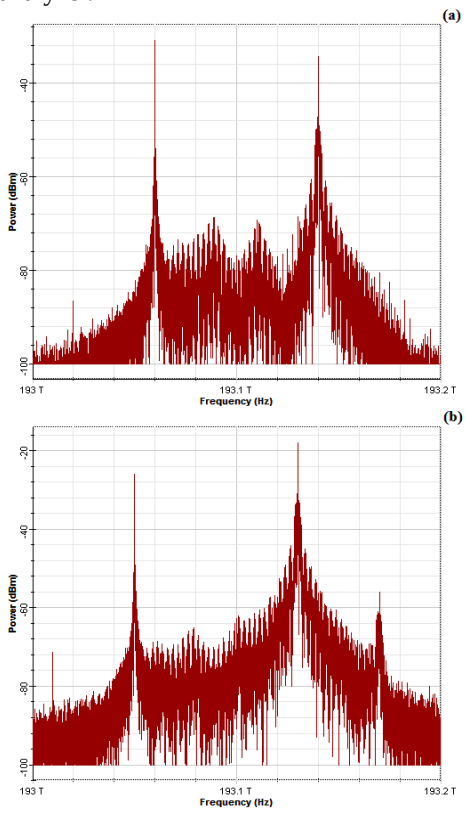

Fig. 2. The optical spectra of the generated optical mm-wave 4PSK signals. (a)DPMZM based, (b) Integrated MZM based

The optical spectra of 4PSK optical MM-wave produced by DPMZM and integrated MZM approaches are given in Fig. 2. We can see from the figure that both the proposed schemes produce optical MM –wave containing two main sidebands spaced at 80 GHz, which is eight times RF driving frequency. As can be seen from Fig. 2(a) that only +4th-order tone carries data while -4th-order tone is un-modulated by data, and it can be found from Fig. 2(b) that only +3rd-order tone is carries data while -5th-order tone is un-modulated by data.

To evaluate system performance of the RoF links based on octupling 4PSK optical MM-wave, BER of DPMZM and integrated MZM based RoF system as a function of received optical power with different transmission distance is shown in Fig. 3(a) and Fig. 3(b), respectively. For the two raised RoF links, the RF power fading and the bit walk-off effects originated from fiber dispersion are restrained availably by the single tone modulation of data signal [13,14], and both schemes have a distribution distance of 30 Km at BER = 10^{-9}. After 30 Km SMF transmission, with BER of 10^{-9}, the receiver sensitivity of DPMZM and integrated MZM based RoF system is about -6 dBm and -2 dBm, respectively. Moreover, MI and corresponding RF driving voltage of RoF system based on DPMZM are lower than those of RoF system based on integrated MZM. These mean that the DPMZM based scheme is superior to the integrated MZM based scheme.

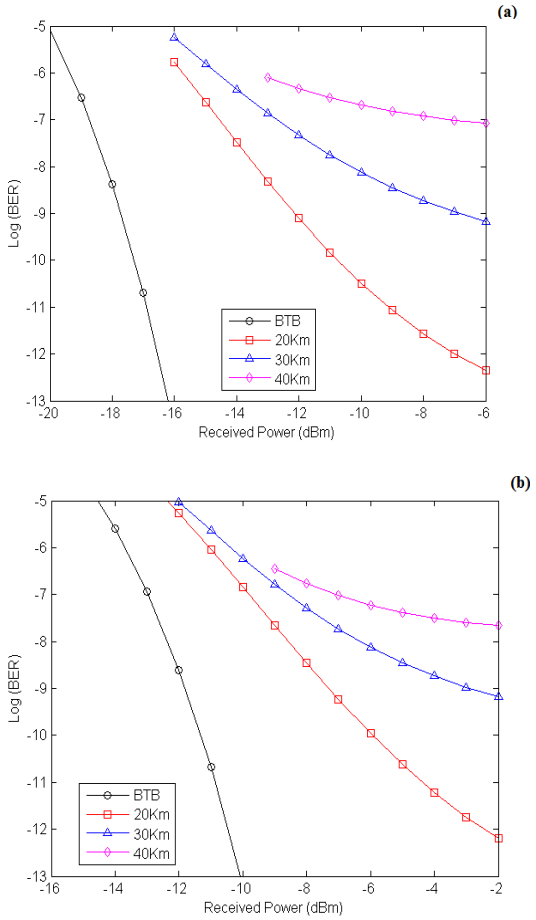

Fig. 3. BER performance of the RoF links for two schemes. (a)DPMZM based, (b) Integrated MZM based (color online)

4. Conclusion

Without optical filtering, two novel frequency octupling schemes based on DPMZM and integrated MZM are devised to produce 4PSK optical MM-wave. Theoretical analysis and simulation experiment are carry out to verify the effectiveness of the two octupling approaches. System performances of 2.5 Gbit/s RoF links based on the outlined approaches are also evaluated, transmission distance of the generated 4PSK optical MM-wave for both schemes can be up to 30 Km at BER = 10^{-9}, and the receiver sensitivity of the DPMZM system gains a advantage over that of the integrated MZM system.

Acknowledgements

This work was supported by National Natural Science Foundation of China (grant # 11603052).

References

[1] J. Yao, Journal of Lightwave Technol. **27**(3), 314 (2009).
[2] N. J. Gomes, A. Nkansah, D. Wake, Journal of Lightwave Technol. **26**(15), 2388 (2008).
[3] A. J. Seeds, K. J. Williams, Journal of Lightwave Technol. **24**(12), 4628 (2006).
[4] Q. Sun, J. Wang, J. Wo, X. Li, D. Liu, Microw. Optical Technol. Lett. **53**(11), 2478 (2011).
[5] Z. Deng, J. Yao, IEEE Trans. Microw. Theory Tech. **54**(2), 763 (2010).
[6] J. Yu, Z. Jia, L. Yi, T. Wang, G. K. Chang, IEEE Photon. Technol. Lett. **19**(19), 1499 (2007).
[7] T. Kawanishi, T. Sakamoto, M. Izutsu, IEEE J. Sel. Topics Quantum Electron. **13**(1), 79 (2007).
[8] X. Chen, L. Xia, D. Huang, Optoelectron. Adv. Mat. **12**(7-8), 455 (2018).
[9] X. Li, S. Zhao, Z. Zhu, B. Gong, Y. Liu, Journal of Modern Optics **62**(18), 1502 (2015).
[10] Z. Zhu, S. Zhao, W. Zheng, W. Wang, B. Lin, Applied Optics **54**(32), 9432 (2015).
[11] M. Li, A. Wen, Y. Chen, L. Shang, L. Yang, Y. Wang, Optics Communications **285**, 5429 (2012).
[12] P. Wu, J. Ma, Optics Communications **374**, 69 (2016).
[13] J. Ma, IEEE/OSA Journal of Optical Communication and Networking **3**(2), 127 (2011).
[14] X. Chen, L. Xia, D. Huang, Optik **147**, 22 (2012).

*Corresponding author: xgchen826@yahoo.com